Built-In Potential in Conjugated Polymer Diodes with Changing Anode Work Function: Interfacial States and Deviation from the Schottky-Mott Limit

ARTICLE *in* JOURNAL OF PHYSICAL CHEMISTRY LETTERS · MAY 2012

Impact Factor: 7.46 · DOI: 10.1021/jz300283h

THE JOURNAL OF PHYSICAL CHEMISTRY Letters

Letter

pubs.acs.org/JPCL

Built-In Potential in Conjugated Polymer Diodes with Changing Anode Work Function: Interfacial States and Deviation from the Schottky–Mott Limit

Bradley A. MacLeod,[†] Noah E. Horwitz,[†] Erin L. Ratcliff,[‡] Judith L. Jenkins,[‡] Neal R. Armstrong,[‡] Anthony J. Giordano,[§] Peter J. Hotchkiss,[§] Seth R. Marder,[§] Charles T. Campbell,[†] and David S. Ginger*[,†]

[†]Department of Chemistry, University of Washington, Seattle, Washington 98195, United States

[‡]Department of Chemistry, University of Arizona, Tucson, Arizona 85721, United States

[§]School of Chemistry and Biochemistry, and Center for Organic Photonics and Electronics, Georgia Institute of Technology, Atlanta, Georgia 30332, United States

Supporting Information

ABSTRACT: We use electroabsorption spectroscopy to measure the change in built-in potential (V_{BI}) across the polymer photoactive layer in diodes where indium tin oxide electrodes are systematically modified using dipolar phosphonic acid self-assembled monolayers (SAMs) with various dipole moments. We find that V_{BI} scales linearly with the work function (Φ) of the SAM-modified electrode over a wide range when using a solution-coated poly(*p*-phenylenevinylene) derivative as the active layer. However, we measure an interfacial parameter of $S = e\Delta V_{BI}/\Delta\Phi < 1$, suggesting that these ITO/SAM/polymer interfaces deviate from the Schottky–Mott limit, in contrast to what has previously been reported for a number of ambient-processed organic-on-electrode systems. Our results suggest that the energetics at these ITO/SAM/polymer interfaces behave more like metal/organic interfaces previously studied in UHV despite being processed from solution.

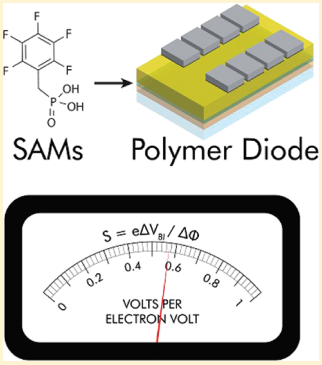

SECTION: Energy Conversion and Storage; Energy and Charge Transport

Solution-processed photovoltaics based on organic semiconductors (OPVs) have the potential to reduce the price of solar photovoltaic electricity generation by reducing materials and manufacturing[1] costs while enabling new flexible and building-integrated form factors that could also reduce the balance of systems costs. Despite these potential benefits, the power conversion efficiency of polymer-based tandem solar cells, currently reported at 10.6% power conversion efficiency for a laboratory test cell,[2] remains below that of more established, commercially available photovoltaic technologies such as Si, CdTe, and copper indium gallium selenide (CIGS).[3] Efforts to better understand OPVs in the hopes of improving performance have thus been the focus of a great deal of research in the past decade.[4−6]

While there is currently some debate about the dominant loss mechanisms in specific OPV devices, several studies have indicated that field-dependent geminate recombination can play a role in many materials systems,[7−16] and many have argued that the collection of photogenerated free charge carriers can depend on a drift field.[17−19] In these cases, understanding the electric field within the organic active layer is important in understanding the photocurrent generation and loss mechanism during device operation. More generally, determination of the internal electric field by measurements of the built-in potential (V_{BI}) across the organic active layer can serve as an indirect probe of the electronic properties of the electrode/organic interfaces that are buried in completed devices.[20,21] Several previous studies have measured V_{BI} in polymer diodes as the work function (Φ) of the contacts was changed.[19,22−28] Additionally, ultraviolet photoelectron spectroscopy (UPS) has been used to measure barrier heights for charge injection from the electrode to organic material, and in all cases where interfaces were formed by depositing an organic onto a metal with at least one of the layers being processed in ambient conditions, Schottky–Mott behavior (vacuum-level alignment between the electrode and organic) was observed.[21] On the other hand, deviations from this limit were observed for a large number of junctions between small-molecule organics deposited on clean metal surfaces (both layers being formed in ultrahigh vacuum without any ambient exposure).[21]

Recently, dipolar phosphonic acids have been used to form self-assembled monolayers (SAMs) on a transparent conducting oxide surface, resulting in shifts in Φ over a range greater than 1 eV.[29] These SAMs have also been shown to improve charge injection and electroluminescence performance in both small-molecule[30] and polymer[31] LEDs. Here, we utilize these

Received: March 9, 2012
Accepted: April 17, 2012
Published: April 17, 2012

phosphonic acids to prepare a series of functionalized indium tin oxide (ITO) electrodes with Φ spanning ~1 eV, and we use electroabsorption spectroscopy to measure the resulting changes in V_{BI} of organic diodes fabricated over the electrodes. There have been few reports that systematically measure differences in V_{BI} for organic diodes as Φ is varied by SAM modification; Smith and co-workers studied thiol-based SAMs (both nonconjugated[32] and π-conjugated[22]) on coinage metal surfaces, and Latini et al.[27] examined the generational growth of poly(amidoamine) on ITO; all observed Schottky–Mott behavior when Φ was within the polymer gap. In contrast, for organic diodes using ITO modified by dipolar phosphonic acid SAMs, we find significant deviations from the Schottky–Mott limit.

Figure 1 shows the structures and abbreviations of the phosphonic acids used in this study, along with Φ of ITO slides

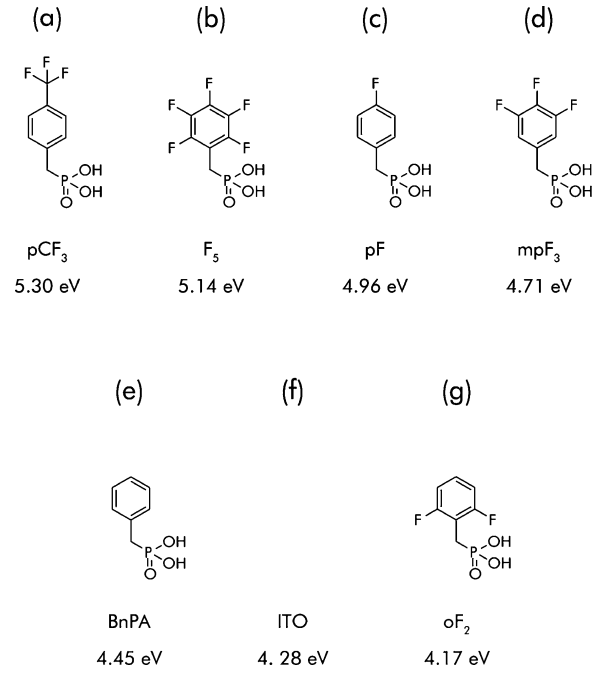

Figure 1. The phosphonic acids used for ITO functionalization with abbreviations and the work function of the (un)modified ITO substrates as measured with low-intensity X-ray photoelectron spectroscopy (Supporting Information): (a) 4-trifluoromethylbenzylphosphonic acid, (b) pentafluorobenzylphosphonic acid, (c) 4-fluorbenzylphosphonic acid, (d) 3,4,5-trifluorobenzylphosphonic acid, (e) benzylphosphonic acid, (f) unmodified ITO control, and (g) 2,6-difluorobenzylphosphonic acid.

modified with each type of SAM. Using monochromatic low-intensity X-ray photoelectron spectroscopy (LIXPS, described in the Supporting Information and elsewhere[33]), we find that these SAMs can be used to adjust the work function of ITO over a window roughly 1.1 eV wide, in qualitative agreement with the work of Hotchkiss et al.[29] In our LIXPS measurements, the absolute Φ's of both our ITO and the SAM-modified ITO were generally smaller in magnitude than those of Hotchkiss et al. by ~0.1–0.3 eV, but these differences are nearly within the uncertainties of the measurement. We observe the same overall trend in relative work function change with phosphonic acid type, as reported by Hotchkiss et al., with the exception of substrates modified with 3,4,5-trifluorobenzylphosphonic acid (mpF3), which consistently produced a smaller Φ relative to the overall trend than was previously reported. We attribute these minor differences both to differences in sample preparation and measurement techniques. Notably, we used a different ITO supplier. We also used a heated submersion SAM deposition method, as compared with the "tethering by growth and aggregation" method[34] used by Hotchkiss et al. Experimentally, we measured Φ's using LIXPS as determined from the point of inflection of the low kinetic energy secondary electron cutoff/step, whereas UPS was used by Hotchkiss et al. Given these differences in methods, we thus conclude that our results are in good relative agreement with previous measurements.

Figure 2a and b shows the poly(*p*-phenylenevinylene) derivative (Super Yellow, SY), as well as the general diode

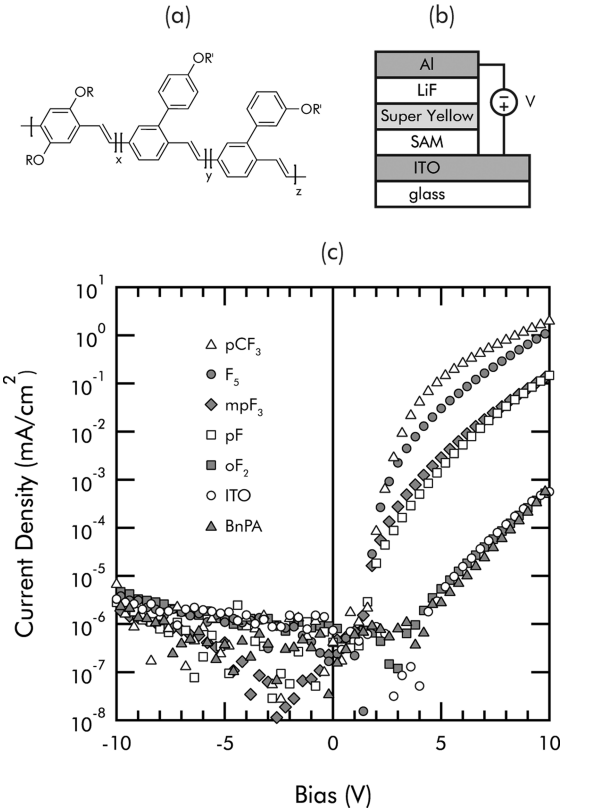

Figure 2. (a) SY polymer structure. (b) SY diode structure (not to scale) used in current–voltage and electroabsorption spectroscopy measurements, with external biasing convention. (c) Dark current–voltage measurements for SY diode measured under low vacuum at room temperature.

structure used in these experiments. Figure 2c shows the current–voltage curves recorded from diodes made using various SAM-modified ITO substrates, a ~100 nm SY active layer, and LiF/Al top contacts. The current–voltage curves show that the four substrates with the largest work functions give progressively larger currents under forward bias. The substrates with the smallest work functions, benzylphosphonic acid (BnPA) on ITO, 2,6-difluorobenzylphosphonic acid (oF_2) on ITO, and unmodified ITO, all exhibited smaller currents and similar injection-limited behavior.

Following current–voltage measurements, we performed electroabsorption measurements to determine the V_{BI}.[20,35] Full details of the experimental method and additional controls can be found in the Supporting Information. Briefly, we applied a

dx.doi.org/10.1021/jz300283h | J. Phys. Chem. Lett. 2012, 3, 1202–1207

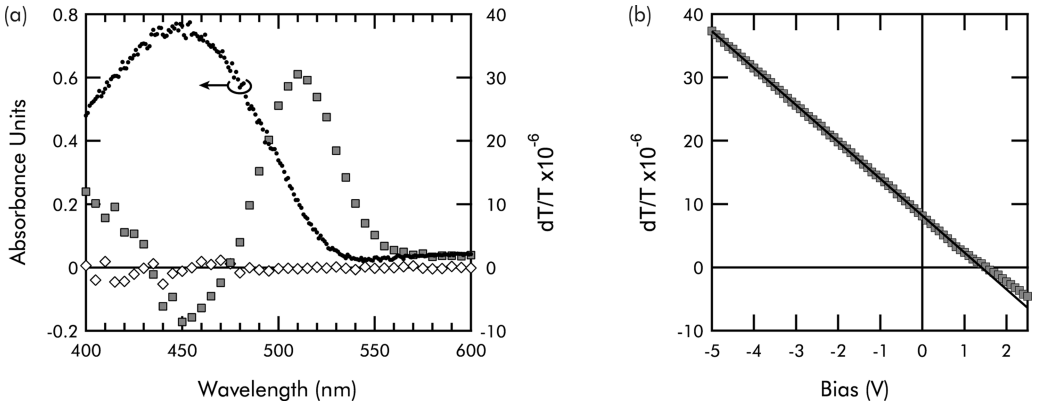

Figure 3. (a) The electroabsorption spectrum (right axis) of a SY diode is shown with the in-phase response (shaded squares) and the negligible quadrature response (white diamonds). For reference, the absorbance (left axis) of the same sample is measured using a UV−vis spectrophotometer, sampling a region where no LiF/Al contacts are present, and blanking with an identically modified ITO substrate. (b) A representative in-phase electroabsorption voltage scan for the same device, with the least-squares linear regression fit to the bias range of −5−0 V is extrapolated through the entire range of the plot. The built-in potential is taken as the linear regression intercept of the *X*-axis. The quadrature response was null and excluded for clarity.

small AC probe voltage, V_{AC}, to the device and illuminated it with a monochromated 75 W Xe arc lamp. Transmitted light was detected at the fundamental AC frequency using lock-in methods to measure the change in transmittance, dT, that is due to the third-order nonlinear susceptibility of the polymer and the applied field. Normalizing by the DC transmittance, T, we obtained the first-harmonic electroabsorption signal, $dT/T \propto (V_{DC} - V_{BI})V_{AC}$, when the polymer was free of added charge carriers.[20] Figure 3a shows a typical electroabsorption spectrum acquired at applied biases of 1 V AC (peak-to-peak) and −5 V DC for the SY film on an ITO substrate with LiF/Al top contacts, along with a UV−vis absorbance of the same film, measured in an area without top contacts. The electroabsorption spectrum has a characteristic derivative line shape, virtually no out-of-phase signal, and negligible absorption in the NIR polaron absorption band, all signs that we are measuring a clean electroabsorption spectrum with minimal interference from charge modulation features.[36−38]

To extract V_{BI} for our SY diodes, we measured the magnitude of the electroabsorption signal as a function of DC bias.[20,35] Generally, the wavelength for this probe is chosen below the polymer gap such that photoinduced charge generation is minimized but the modulated response is still significant. Figure 3b shows the DC voltage response at 1 V AC and a constant wavelength of 528 nm for the same device as that in Figure 3a. We extract V_{BI} by performing a linear fit to the data in the reverse bias range, as indicated in the figure, and extrapolate V_{BI} from the intercept. We have found that this procedure minimizes interference from charge injection near flat band conditions, which can lead to deviations in linearity at DC biases close to V_{BI}, as has been reported to complicate some studies.[36] Using this approach, we measured V_{BI} for a series of diodes prepared on each SAM-modified ITO substrate.

The data in Figure 4 show a linear trend with an apparent onset of saturation at the highest substrate work function; we observe a monotonic increase in V_{BI} as the work function of the substrate is increased over the range from 4.17 to 5.14 eV, but the V_{BI}'s for the substrates with the two highest work functions are the same (∼2.00 V) within experimental error. We attribute this break in the linear trend at high Φ's to the Fermi-level pinning that has been reported in many metal−semiconductor interface studies as the Φ of the metal approaches the highest-

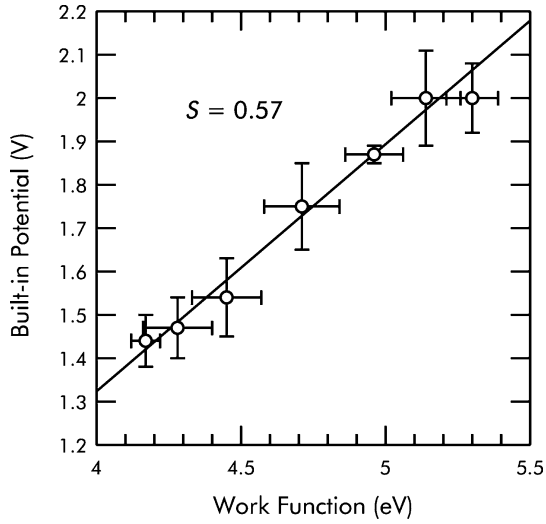

Figure 4. Mean V_{BI} of ITO/SAM/SY/LiF/Al diodes versus the mean Φ of ITO/SAM surfaces (prepared in the same batch as one of the batches of diodes used for electroabsorption) with vertical and horizontal error bars representing the standard deviation of the mean. Mean V_{BI} was taken from three or more pixels in each of two identically prepared batches of ITO/SAM/SY/LiF/Al diodes. The mean Φ was taken from five spots on two or more samples of ITO/SAM surfaces (prepared in the same batch as one of the batches of diodes used for electroabsorption). A linear regression that omits the highest work function (due to presumed Fermi-level pinning) is shown with the magnitude of the slope, *S*.

occupied molecular orbital (HOMO) of the semiconductor.[21,39] Our UPS measurements of the ionization potential of SY put the HOMO at 5.7 ± 0.1 eV (Supporting Information). The data in Figure 4 are thus consistent with Fermi-level pinning occurring roughly 0.5 eV above the SY HOMO edge. Fermi-level pinning of the electrode several tenths of an eV above the HOMO edge has been observed previously in many organic semiconductors and is generally attributed to charge transfer to the tail of the density of states[21,40] within the gap. The straight line in Figure 4 is a linear fit to the data with slope = 0.57. In the Schottky−Mott limit, when the dielectric layer is free of charge carriers, V_{BI} changes with the electrode Φ with a unity slope. The subunity slope obtained here thus indicates a

dx.doi.org/10.1021/jz300283h | *J. Phys. Chem. Lett.* 2012, 3, 1202−1207

deviation from this limit for the interface between the SAM-modified ITO and the polymer, which contrasts with the previous reports of V_{BI} made using electroabsorption on a series of SAM-modified electrodes[22,32] and more generally with the trend that "dirty" (e.g., non-UHV) solution-processed electrode−organic interfaces tend to exhibit Schottky−Mott behavior.[21] We note that although a subunity slope has also been observed for polymer devices prepared with reactive and/or interdiffusing top contacts that may induce deep gap states at the interface,[21,24] this mechanism is likely distinct from the effects studied here at the presumed nonreactive, SAM-modified ITO bottom contacts.

The observed subunity slope could be explained by a number of possible physical models. For instance, the induced density of interface states (IDIS) model[41,42] indicates that a density of states within the semiconductor gap equal to $\sim 5 \times 10^{13}$ cm^{-2} is sufficient to bring the slope/proportionality between V_{BI} and Φ below unity as the slope S is inversely proportional to the density of interface states.[21] While the origin of such states is an open question, the states do not appear to be intrinsic to the SY polymer (we also observed deviation from the Schottky−Mott limit for a polyfluorene, Supporting Information). We note that the density of states required to observe a subunity slope is on the order of the SAM coverage density on ITO for the Φ that we measure here (previously estimated to be 2×10^{13} to 1×10^{14} cm^{-2}),[29,43] suggesting a role of the SAM molecules in the interfacial state formation. We speculate that the fluorinated SAM may serve to reduce atmospheric/process contamination prior to the polymer being spin-coated and that the relatively thin SAM layer does not inhibit electronic overlap between electronic states in the ITO and a density of interface states in the organic. Alternatively, we speculate that the phosphonic acids used here may form $\pi-\pi$ interactions with the conjugated polymers. Finally, we note that the strong dipole interactions of the SAM layer could influence the solid-state order of the first monolayer of solution-processed polymers during spin-coating, leading to an oriented interface layer with a partially counteracting dipole. Further detailed experiments will be required to distinguish between these hypotheses.

We used a class of dipolar, fluorine-substituted benzylphosphonic acids to modify Φ of ITO electrodes. Using electroabsorption spectroscopy, we measured V_{BI} in a series of conjugated polymer diodes formed on these SAMs. Interfaces formed by solution coating a poly(*p*-phenylenevinylene) derivative onto ITO/SAM surfaces displayed clear deviation from the Schottky−Mott limit, which is distinct from most previous reports of electrode−organic interfaces in which the underlying electrode has undergone ambient exposure prior to the organic deposition.[21] These results demonstrate that phosphonic acid SAMs could be used to tailor performance by increasing V_{BI} in solution-processed polymer light-emitting diodes or solar cells and that interfaces exhibiting electronic behavior similar to that observed under UHV conditions can also be observed with simple ambient solution processing.

EXPERIMENTAL METHODS

Samples Preparation. ITO was from Thin Film Devices Inc. (Eagle XG, 145 nm thickness, 0.7 nm rms surface roughness, 20 ± 2 Ω/□). ITO substrates were etched with 25 mg/mL Zn in 1 M hydrochloric acid to leave a 9 mm wide stripe of ITO, centered on the 15 mm × 15 mm glass substrate. Substrates were then scrubbed with isopropyl alcohol, scrubbed with detergent solution (2 vol % Micro-90, International Products Corporation, in purified deionized water), and then ultrasonicated in detergent solution, purified deionized water, and neat ethanol for 10 min each. Substrates were then oxygen plasma cleaned (Harrick Plasma HDC-32G, 6.8 W power setting) for 10 min with the oxygen flow rate metered at 100 mL/min. Substrates were immediately submersed and sealed in a reaction vial at 75 °C and incubated for 48 h. For the ITO control, the vial contained neat ethanol; the others each contained a 10 mM ethanolic solution of the phosphonic acid molecules shown in Figure 1 (with syntheses being previously reported[29,44]). Substrates were rinsed in copious amounts of neat ethanol, such that no residual materials were visible, and then dried with nitrogen gas. Substrates were further dried under low vacuum at 140 °C for 2 h. Substrates that were characterized with LIXPS were treated similarly up to this point, with the exception that the initial substrates were smaller and were not etched. Diode substrates were vented to a nitrogen glovebox atmosphere for spin-coating (<5 PPM oxygen and <0.1 PPM water). SY (EMD Chemicals PDY-132, proposed structure[45] shown in Figure 2a), 6 mg/mL neat anhydrous toluene, was spincoated from 45 °C, resulting in 103 nm thick films (measured with a Tencor Alpha-Step 500 surface profiler). Films were directly loaded into a gloevbox-integrated thermal evaporator (Angstrom Engineering Åmod 600 series) with a shadow mask to deposit 7 Å of LiF at 0.1 Å/s and a pressure < 5×10^{-7} Torr, defining 8 pixels per substrate with an active area of approximately 4.2 mm^2 each. The chamber was vented to the glovebox atmosphere to exchange the LiF source with an Al source to minimize cross-shadowing effects, and 100 nm of Al was deposited at 1 Å/s and a pressure < 5×10^{-7} Torr. The devices were kept under static vacuum.

Diode Experiments. Conductive silver paint was applied to the Al contacts above the etched area of the underlying substrate (nonactive area) to provide more reliable contact to the test pins. The device was transferred to the optical table sealed in the test chamber under a nitrogen atmosphere, where a low-vacuum system pumped on the sample during testing, such that the device was never exposed to atmospheric conditions. External bias was applied to the common ITO contact with the reference potential applied to the silver-painted Al contact, as indicated in Figure 2b. For the devices in this study, a forward-bias current conditioning was implemented in which devices underwent an irreversible change leading to current−voltage characteristics that were reproducible upon subsequent scans (Supporting Information). Current−voltage characteristics were recorded for each pixel with the device shielded from light. Electroabsorption spectroscopy was performed with the probe beam incident at 45° from the surface normal of the glass−vacuum interface of the device, and light that is not absorbed in the polymer active layer was reflected at the back electrode and collected at 90° from the angle of incidence. During the measurement, a potential was applied to the common ITO electrode from a summation of DC (Keithley 2400) and AC (Agilent 33210A) voltages. See Supporting Information Figures S3 and S4 for the experimental schematic and photographs of the apparatus. In our lab, the peak signal-to-noise ratio was found to occur with the AC modulation at around 4 kHz and was used for all measurements reported here. Transmitted light was collected with a silicon photodetector (Thorlabs FDS1010) and the current preamplified (Stanford Research SR570), with output DC and AC photovoltages being measured simultaneously by a Keithley 2400 and the AC

dx.doi.org/10.1021/jz300283h | *J. Phys. Chem. Lett.* 2012, 3, 1202−1207

voltage input of a lock-in amplifier (Stanford Research SR830), respectively. The ratio of AC to DC response, dT/T, normalizes for the system response function.

■ ASSOCIATED CONTENT

Supporting Information

Additional notes on sample preparation, diode conditioning, electroabsorption spectroscopy, V_{BI} in other polymer systems, LIXPS, and UPS. This material is available free of charge via the Internet at http://pubs.acs.org.

■ AUTHOR INFORMATION

Corresponding Author

*E-mail: ginger@chem.washington.edu.

Notes

The authors declare no competing financial interest.

■ ACKNOWLEDGMENTS

This work is supported as part of the Center for Interface Science: Solar Electric Materials (CISSEM), an Energy Frontier Research Center funded by the U.S. Department of Energy, Office of Science, Office of Basic Energy Sciences, under Award Number DE-SC0001084. Prof. Fumio S. Ohuchi, Prof. Marjorie A. Olmstead, and The Micron Foundation supported the use of the XPS instrument. B.A.M. performed early parts of this research as a NSF Graduate Research Fellow. N.E.H. was supported by a Washington Research Foundation/NASA Space Grant Fellowship during part of this work. A.J.G.'s work was supported by a NSF Graduate Research Fellowship and a National Defense Science and Engineering Graduate Fellowship.

■ REFERENCES

(1) Krebs, F. C. Fabrication and Processing of Polymer Solar Cells: A Review of Printing and Coating Techniques. *Sol. Energy Mater. Sol. Cells* **2009**, *93*, 394−412.

(2) Kromhout, W. W. *UCLA Engineers Create Tandem Polymer Solar Cells that Set Record for Energy-conversion*; UCLA Newsroom: Los Angeles, CA, 2012.

(3) Green, M. A.; Emery, K.; Hishikawa, Y.; Warta, W.; Dunlop, E. D. Solar Cell Efficiency Tables (version 39). *Prog. Photovolt: Res. Appl.* **2012**, *20*, 12−20.

(4) Groves, C.; Reid, O. G.; Ginger, D. S. Heterogeneity in Polymer Solar Cells: Local Morphology and Performance in Organic Photovoltaics Studied with Scanning Probe Microscopy. *Acc. Chem. Res.* **2010**, *43*, 612−620.

(5) Giridharagopal, R.; Ginger, D. S. Characterizing Morphology in Bulk Heterojunction Organic Photovoltaic Systems. *J. Phys. Chem. Lett.* **2010**, *1*, 1160−1169.

(6) Servaites, J. D.; Ratner, M. A.; Marks, T. J. Organic Solar Cells: A New Look at Traditional Models. *Energy Environ. Sci.* **2011**, *4*, 4410−4422.

(7) Andersson, L. M.; Müller, C.; Badada, B. H.; Zhang, F.; Würfel, U.; Inganäs, O. Mobility and Fill Factor Correlation in Geminate Recombination Limited Solar Cells. *J. Appl. Phys.* **2011**, *110*, 024509.

(8) Lee, J.; Vandewal, K.; Yost, S. R.; Bahlke, M. E.; Goris, L.; Baldo, M. A.; Manca, J. V.; Voorhis, T. V. Charge Transfer State Versus Hot Exciton Dissociation in Polymer−Fullerene Blended Solar Cells. *J. Am. Chem. Soc.* **2010**, *132*, 11878−11880.

(9) Pal, S. K.; Kesti, T.; Maiti, M.; Zhang, F.; Inganäs, O.; Hellström, S.; Andersson, M. R.; Oswald, F.; Langa, F.; Österman, T.; et al. Geminate Charge Recombination in Polymer/Fullerene Bulk Heterojunction Films and Implications for Solar Cell Function. *J. Am. Chem. Soc.* **2010**, *132*, 12440−12451.

(10) Howard, I. A.; Mauer, R.; Meister, M.; Laquai, F. Effect of Morphology on Ultrafast Free Carrier Generation in Polythiophene:-Fullerene Organic Solar Cells. *J. Am. Chem. Soc.* **2010**, *132*, 14866−14876.

(11) Giebink, N. C.; Lassiter, B. E.; Wiederrecht, G. P.; Wasielewski, M. R.; Forrest, S. R. Ideal Diode Equation for Organic Heterojunctions. II. The Role of Polaron Pair Recombination. *Phys. Rev. B* **2010**, *82*, 155306.

(12) Müller, J.; Lupton, J.; Feldmann, J.; Lemmer, U.; Scharber, M.; Sariciftci, N.; Brabec, C.; Scherf, U. Ultrafast Dynamics of Charge Carrier Photogeneration and Geminate Recombination in Conjugated Polymer:Fullerene Solar Cells. *Phys. Rev. B* **2005**, *72*, 195208.

(13) Offermans, T.; van Hal, P.; Meskers, S.; Koetse, M.; Janssen, R. Exciplex Dynamics in a Blend of π-Conjugated Polymers with Electron Donating and Accepting Properties: MDMO-PPV and PCNEPV. *Phys. Rev. B* **2005**, *72*, 045213.

(14) Peumans, P.; Forrest, S. R. Separation of Geminate Charge-Pairs at Donor−Acceptor Interfaces in Disordered Solids. *Chem. Phys. Lett.* **2004**, *398*, 27−31.

(15) Mihailetchi, V. D.; Koster, L. J. A.; Hummelen, J. C.; Blom, P. W. M. Photocurrent Generation in Polymer−Fullerene Bulk Heterojunctions. *Phys. Rev. Lett.* **2004**, *93*, 216601.

(16) Ramsdale, C. M.; Barker, J. A.; Arias, A. C.; MacKenzie, J. D.; Friend, R. H.; Greenham, N. C. The Origin of the Open-Circuit Voltage in Polyfluorene-Based Photovoltaic Devices. *J. Appl. Phys.* **2002**, *92*, 4266−4270.

(17) Koster, L. J. A.; Smits, E. C. P.; Mihailetchi, V. D.; Blom, P. W. M. Device Model for the Operation of Polymer/Fullerene Bulk Heterojunction Solar Cells. *Phys. Rev. B* **2005**, *72*, 085205.

(18) Mozer, A.; Dennler, G.; Sariciftci, N.; Westerling, M.; Pivrikas, A.; Österbacka, R.; Juška, G. Time-Dependent Mobility and Recombination of the Photoinduced Charge Carriers in Conjugated Polymer/Fullerene Bulk Heterojunction Solar Cells. *Phys. Rev. B* **2005**, *72*, 035217.

(19) Zimmermann, B.; Glatthaar, M.; Niggemann, M.; Riede, M.; Hinsch, A. Electroabsorption Studies of Organic Bulk-Heterojunction Solar Cells. *Thin Solid Films* **2005**, *493*, 170−174.

(20) Brown, T. M.; Cacialli, F. In *Conjugated Polymers: Theory, Synthesis, Properties, and Characterization*; Skotheim, T. A., Reynolds, J. R., Eds.; CRC Press: Boca Raton, FL, 2007.

(21) Hwang, J.; Wan, A.; Kahn, A. Energetics of Metal−Organic Interfaces: New Experiments and Assessment of the Field. *Mater. Sci. Eng., R* **2009**, *64*, 1−31.

(22) Campbell, I. H.; Rubin, S.; Zawodzinski, T. A.; Kress, J. D.; Martin, R. L.; Smith, D. L.; Barashkov, N. N.; Ferraris, J. P. Controlling Schottky Energy Barriers in Organic Electronic Devices Using Self-Assembled Monolayers. *Phys. Rev. B* **1996**, *54*, R14321−R14324.

(23) Brown, T. M.; Friend, R. H.; Millard, I. S.; Lacey, D. J.; Burroughes, J. H.; Cacialli, F. LiF/Al Cathodes and the Effect of LiF Thickness on the Device Characteristics and Built-in Potential of Polymer Light-Emitting Diodes. *Appl. Phys. Lett.* **2000**, *77*, 3096−3098.

(24) Brown, T. M.; Friend, R. H.; Millard, I. S.; Lacey, D. J.; Butler, T.; Burroughes, J. H.; Cacialli, F. Electronic Line-up in Light-Emitting Diodes with Alkali-Halide/Metal Cathodes. *J. Appl. Phys.* **2003**, *93*, 6159−6172.

(25) Morgado, J.; Barbagallo, N.; Bodrozic, V.; Teixeira, A.; Femandes, A. C.; Giintner, R.; Scherf, U.; Cacialli, F.; Alcacer, L. Indium-Tin Oxide Anodes Modified by Self-Assembly for Light-Emitting Diodes Based on Blue-Emitting Polyfluorenes. *Synth. Met.* **2005**, *154*, 153−156.

(26) Morgado, J.; Barbagallo, N.; Charas, A.; Matos, M.; Alcácer, L. s; Cacialli, F. Self-Assembly Surface Modified Indium Tin Oxide Anodes for Single-Layer Light-Emitting Diodes. *J. Phys. D: Appl. Phys.* **2003**, *36*, 434−438.

(27) Latini, G.; Wykes, M.; Schlapak, R.; Howorka, S.; Cacialli, F. Self-Assembled Monolayers of Protonated Poly(amidoamine) Dendrimers on Indium Tin Oxide. *Appl. Phys. Lett.* **2008**, *92*, 013511.

(28) Hoven, C. V.; Peet, J.; Mikhailovsky, A.; Nguyen, T. Q. Direct Measurement of Electric Field Screening in Light Emitting Diodes with Conjugated Polyelectrolyte Electron Injecting/Transport Layers. *Appl. Phys. Lett.* **2009**, *94*, 033301.
(29) Hotchkiss, P. J.; Li, H.; Paramonov, P. B.; Paniagua, S. A.; Jones, S. C.; Armstrong, N. R.; Brédas, J.-L.; Marder, S. R. Modification of the Surface Properties of Indium Tin Oxide with Benzylphosphonic Acids: A Joint Experimental and Theoretical Study. *Adv. Mater.* **2009**, *21*, 4496−4501.
(30) Sharma, A.; Hotchkiss, P. J.; Marder, S. R.; Kippelen, B. Tailoring the Work Function of Indium Tin Oxide Electrodes in Electrophosphorescent Organic Light-Emitting Diodes. *J. Appl. Phys.* **2009**, *105*, 084507.
(31) Knesting, K. M.; Hotchkiss, P. J.; MacLeod, B. A.; Marder, S. R.; Ginger, D. S. Spatially Modulating Interfacial Properties of Transparent Conductive Oxides: Patterning Work Function with Phosphonic Acid Self-Assembled Monolayers. *Adv. Mater.* **2012**, *24*, 642−646.
(32) Campbell, I. H.; Kress, J. D.; Martin, R. L.; Smith, D. L.; Barashkov, N. N.; Ferraris, J. P. Controlling Charge Injection in Organic Electronic Devices Using Self-Assembled Monolayers. *Appl. Phys. Lett.* **1997**, *71*, 3528−3530.
(33) Schlaf, R.; Murata, H.; Kafafi, Z. H. Work Function Measurements on Indium Tin Oxide Films. *J. Electron Spectrosc. Relat. Phenom.* **2001**, *120*, 149−154.
(34) Paniagua, S. A.; Hotchkiss, P. J.; Jones, S. C.; Marder, S. R.; Mudalige, A.; Marrikar, F. S.; Pemberton, J. E.; Armstrong, N. R. Phosphonic Acid Modification of Indium−Tin Oxide Electrodes: Combined XPS/UPS/Contact Angle Studies. *J. Phys. Chem. C* **2008**, *112*, 7809−7817.
(35) Campbell, I. H.; Hagler, T. W.; Smith, D. L.; Ferraris, J. P. Direct Measurement of Conjugated Polymer Electronic Excitation Energies Using Metal/Polymer/Metal Structures. *Phys. Rev. Lett.* **1996**, *76*, 1900−1903.
(36) de Vries, R. J.; van Mensfoort, S. L. M.; Janssen, R. A. J.; Coehoorn, R. Relation Between the Built-in Voltage in Organic Light-Emitting Diodes and the Zero-Field Voltage as Measured by Electroabsorption. *Phys. Rev. B* **2010**, *81*, 125203.
(37) Zhou, M.; Chua, L.-L.; Png, R.-Q.; Yong, C.-K.; Sivaramakrishnan, S.; Chia, P.-J.; Wee, A. T. S.; Friend, R. H.; Ho, P. K. H. Role of δ-Hole-Doped Interfaces at Ohmic Contacts to Organic Semiconductors. *Phys. Rev. Lett.* **2009**, *103*, 036601.
(38) Brewer, P. J.; deMello, A. J.; deMello, J. C.; Lane, P. A.; Bradley, D. D. C.; Fletcher, R.; O'Brien, J. Influence of Carrier Injection on the Electromodulation Response of Trap-Rich Polymer Light-Emitting Diodes. *J. Appl. Phys.* **2006**, *99*, 114502.
(39) Tengstedt, C.; Osikowicz, W.; Salaneck, W. R.; Parker, I. D.; Hsu, C.-H.; Fahlman, M. Fermi-Level Pinning at Conjugated Polymer Interfaces. *Appl. Phys. Lett.* **2006**, *88*, 053502.
(40) Blakesley, J. C.; Greenham, N. C. Charge Transfer at Polymer-Electrode Interfaces: The Effect of Energetic Disorder and Thermal Injection on Band Bending and Open-Circuit Voltage. *J. Appl. Phys.* **2009**, *106*, 034507.
(41) Vázquez, H.; Flores, F.; Kahn, A. Induced Density of States Model for Weakly-Interacting Organic Semiconductor Interfaces. *Org. Electron.* **2007**, *8*, 241−248.
(42) Mönch, W. On the Physics of Metal−Semiconductor Interfaces. *Rep. Prog. Phys.* **1990**, *53*, 221−278.
(43) Li, H.; Paramonov, P.; Bredas, J.-L. Theoretical Study of the Surface Modification of Indium Tin Oxide with Trifluorophenyl Phosphonic Acid Molecules: Impact of Coverage Density and Binding Geometry. *J. Mater. Chem.* **2010**, *20*, 2630−2637.
(44) Hotchkiss, P. J. *The Design, Synthesis, and Use of Phosphonic Acids for the Surface Modification of Metal Oxides*; Georgia Institute of Technology: Atlanta, GA, 2008.
(45) Edman, L.; Summers, M. A.; Buratto, S. K.; Heeger, A. J. Polymer Light-Emitting Electrochemical Cells: Doping, Luminescence, and Mobility. *Phys. Rev. B* **2004**, *70*, 115212.